Dating late Holocene lava flows in Pico de Orizaba (Mexico) by means of in situ-produced cosmogenic 36Cl, lichenometry and dendrochronology

Jesús Alcalá-Reygosa, David Palacios, Irene Schimmelpfennig, Lorenzo
Vázquez-Selem, Leopoldo García-Sancho, Osvaldo Franco-Ramos, José
Villanueva, José Juan Zamorano, Georges Aumaitre, Didier Bourles, et al.

HAL Id: hal-01795226
https://hal.science/hal-01795226

Submitted on 3 May 2019

Dating late Holocene lava flows in Pico de Orizaba (Mexico) by means of *in situ*-produced cosmogenic [36]Cl, lichenometry and dendrochronology

Jesús Alcalá-Reygosa[a,*], David Palacios[b], Irene Schimmelpfennig[c], Lorenzo Vázquez-Selem[d], Leopoldo García-Sancho[e], Osvaldo Franco-Ramos[d], José Villanueva[f], José Juan Zamorano[d], ASTER Team (Georges Aumaître[g], Didier Bourlès[g], Karim Keddadouche[g])

[a] *Facultad de Filosofía y Letras, Universidad Nacional Autónoma de México, Ciudad Universitaria, 04510 Ciudad de México, Mexico*

[b] *Departamento de Geografía, Facultad de Geografía e Historia, Universidad Complutense, C/ Profesor Aranguren S/N, 28040, Madrid, Spain*

[c] *Aix Marseille Univ, CNRS, IRD, INRA, Coll France, CEREGE, Aix-en-Provence, France*

[d] *Instituto de Geografía, Universidad Nacional Autónoma de México, Ciudad Universitaria, 04510 Ciudad de México, Mexico*

[e] *Departamento de Biología Vegetal II, Facultad de Farmacia, Universidad Complutense, Plaza de Ramón y Cajal S/N, Ciudad Universitaria, 28040, Madrid, Spain*

[f] *INIFAP CENID-RASPA, Km 6,5 Margen Derecha del Canal Sacramento, Gómez Palacio, Durango, Mexico*

[g] *Aix Marseille Univ, CNRS, IRD, INRA, Coll France, CEREGE, Aix-en-Provence, France*

A B S T R A C T

The knowledge of the eruptive history of volcanic centers allows for improving the evaluation of the related risks and hazards in populated areas, but substantially depends on the ability of dating the lava flows. However, traditional methods such as U-Th/He, ^{40}Ar-^{39}Ar, ^{40}K-^{40}Ar and radiocarbon dating are not always suitable. Therefore, an alternative approach based on the combination of *in situ*-produced ^{36}Cl based cosmic ray exposure dating, lichenometry and dendrochronology was tested on two lava flows (called Lava flow "A" and "B") from Pico de Orizaba (Mexico), previously attributed to 16th and 17th century eruptions, respectively. The presented results show that both lava flows are significantly older than their assumed 16th and 17th century ages. Regarding lava flow "A", the measured *in situ*-produced ^{36}Cl concentrations lead to a mean age of 3.03 ± 0.70 ka, while dendrochronology and lichenometry yield minimum ages of 834 and 1130 years, respectively. Regarding lava flow "B", the measured *in situ*-produced ^{36}Cl concentrations lead to a mean age of 1.45 ± 0.35 ka, whereas lichenometry gives a minimum age of ~1000 years. Overall, this demonstrates that the combination of *in situ*-produced ^{36}Cl based cosmic ray exposure dating, lichenometry and dendrochronology has a con- siderable potential for dating purposes on young deposits and landforms, in particular on lava flows at high elevation sites.

1. Introduction

Dating lava flows provides new insights into the eruptive history of volcanic centers such as stratovolcanoes, thus allowing for the estima- tion of the related hazards and risks in populated areas. In this sense, dating lava flows over time scales covering the last centuries to the last millennia is important to test models that aim at establishing potential patterns of eruption recurrence and thus to improve the prediction of future eruptions. Moreover, some stratovolcanoes are ice-capped, and better understanding their glacio-volcanic evolution helps evaluating the hazards related to the interaction between ice and volcanic activity (i. e. large debris flows and floods) (Lescinsky and Fink, 2000; Conway et al., 2015; Heineke et al., 2016).

Several methods can be used to date Quaternary lava flows, in- cluding ^{40}Ar-^{39}Ar (Wijbrans et al., 2011; Conway et al., 2015), ^{40}K-^{40}Ar (Germa et al., 2010) radiocarbon (Calvert et al., 2006) and U-Th/He dating (Aciego et al., 2007). However, most of these techniques tend to be unsuitable to date lava flows that were emplaced during the Late Holocene, i.e. during the past 4–5 ka. The ^{40}Ar-^{39}Ar and ^{40}K-^{40}Ar dating methods require a detectable concentration of ^{40}Ar (Renne, 2000). Due to its relatively short half-life of 5730 years, radiocarbon can only be used to date lava flows that were emplaced less than ~50 ka ago. However, for this dating technique, organic material in association with the lava flows is required, which is not always available, especially at high elevations where vegetation is scarce. Nonetheless, radiocarbon dating remains the most commonly used method over this time scale (Trumbore, 2000). The U-Th/He dating method is suitable for dating Late Holocene volcanic rocks, but relies on the presence of atypical volcanic minerals such as garnet, zircon and fayalite with U-rich con- centrations (Aciego et al., 2007). Therefore, alternative methods are needed to determine the age of young lava flows.

Comic ray exposure (CRE) dating, based on measurements of the concentration of *in situ*-produced cosmogenic nuclides such as ber- yllium-10 (^{10}Be), chlorine-36 (^{36}Cl) and helium-3 (^{3}He) in terrestrial surface samples, constitutes a robust method to establish chronological constraints on landform processes (Dunai, 2010). This dating technique relies on the interaction of cosmic ray derived particles with certain target elements in the minerals of the Earth's surface, resulting in steady accumulation of various rare isotopes (*in situ* in the crystal lattice) with time. The method offers various advantages over others including that it is applicable to time scales between 10^2 and 10^6 years, depending on the preservation state of the lava surface and to a wide range of common rock types and minerals that are present at the Earth's surface.
I. e. ^{10}Be is produced in quartz and can thus be used to date any quartz-bearing lithology; ^{36}Cl is produced in any K- and Ca-bearing rocks and minerals and can thus be used to date feldspars, pyroxenes and car- bonates; and ^{3}He can be extracted from olivines, pyroxenes and horn- blendes. To obtain accurate CRE ages, accurate production rates and scaling schemes are required (Dunai, 2010).

As quartz is rarely present in volcanic rocks and ^{10}Be is therefore generally not suited to date lava flows, the measurements of ^{3}He, ^{21}Ne or ^{36}Cl in lava flow surfaces are most adequate for dating their em- placements, the choice of the nuclide mostly depending on the rock's mineralogy. In addition, it has been shown that these techniques lead to consistent Holocene ages for the studied volcanic eruptions (Dunbar, 1999; Foeken et al., 2009; Espanon et al., 2014; Fenton and Niedermann, 2014). While ^{3}He and ^{21}Ne have specifically to be ana- lyzed in the pyroxene and olivine phenocrysts of mafic lavas, ^{36}Cl can be extracted from any mineral phase and rock type that contains one or more of its most important target elements, i.e. Ca, K and Cl. Moreover, it has been recently shown that reliable ^{36}Cl CRE ages as young as a few hundred years can be obtained for volcanic rocks (Jomelli et al., 2016). Although ^{36}Cl analysis in specific Ca- and/or K-rich minerals, such as feldspars or clinopyroxenes, is preferable to that in volcanic whole rocks because this

approach generally allows minimizing the Cl con- centrations that are often very high in the lava matrix (Schimmelpfennig et al., 2009), the absence of sufficient phenocrysts in the lava flows to be dated in this study prevented us to analyze ^{36}Cl in mineral separates. Instead, we used whole rocks to estimate the em- placement age of the lava flows.

Late Holocene lava flows that are exposed at the surface are parti- cularly well suited for CRE dating, because their exposure history is simple and the original surface features are often well preserved al- lowing to reduce the impact of erosion and exhumation on the nuclide inventory (Espanon et al., 2014; Fenton and Niedermann, 2014; Kurz et al., 2014; Medynski et al., 2015; Heineke et al., 2016). Moreover, as lava flows are static surfaces, they are not affected by nuclide in- heritance from previous exposure (Dunai, 2010; Dunai et al., 2014). Due to these advantages, lava flows with ages between 0.4 and up to 250 ka have also been used to obtain ^{3}He and ^{36}Cl production rates (e.g. Cerling, 1990; Schimmelpfennig et al., 2011; Foeken et al., 2012; Schneider et al., 2014).

Dendrochronology and lichenometry are also surface dating methods, based on the start time of colonization by the living organism, which however can lag behind the timing of rock surface formation by an unknown period of time. Therefore, these methods only provide minimum ages and are limited by the organisms' life spans, i.e. gen- erally to the past few hundred years. Dendrochronology is based on the dating of growth rings of woody plants. It has been used for the de- termination of minimum ages of Late Holocene geomorphic surfaces (Shroder and Butler, 1987; Stoffel et al., 2010), including volcano-flu- vial terraces (Pierson, 2007) and post-eruptive ravines (Franco-Ramos et al., 2017). In the mountains of central Mexico, the pine species forming the timberline, *Pinus hartwegii*, can reach ages of > 500 yr (Villanueva-Díaz et al., 2015). In addition, the alpine juniper shrub *Juniperus monticola*, which forms annual rings, can live > 800 years and has high dendrochronological potential (Villanueva-Díaz et al., 2016). Lichenometry is based on a known growth rate of the thalli of li- chens. It has been used since the 1960s for surface dating (Armstrong, 2016). The species *Rhizocarpon geographicum* has frequently been used because it grows on most of the Earth's mountains and in both circum- polar regions. It exhibits a slow and constant growth rate (Bradwell and Armstrong, 2007). Thus, lichenometry has been widely applied to date glacial and alluvial deposits, slope processes, surfaces affected by tectonics, archeological sites, etc. (Bull, 2015). It is the technique most usually employed to date Late Holocene glacial landforms (Briner, 2011). However, lichenometry has been less used to date volcanic landforms such as lava flows (Clarkson and Clarkson, 1983; Angiel and Dąbski, 2012), lahars and debris avalanches (Crandell et al., 1974), although several studies of lichen colonization have been performed to establish the growth curve on lava flows in tropical (Kurina and Vitousek, 1999), subtropical (Mancebo et al., 1989), temperate (Shimizu, 2004) and polar environments (Talbot et al., 2010). More- over, lichenometry has been combined with other dating methods such as tephrochronology (Beget, 1984; Kirkbride and Dugmore, 2008), radiocarbon dating (Beget, 1984) and dendrochronology (Koch et al., 2007) in volcanic environments to control their surface ages.

Here, we test the combination of the *in situ*-produced ^{36}Cl based cosmic ray exposure dating (hereafter ^{36}Cl CRE dating), lichenometry and dendrochronology dating methods to determine the age of two young lava flows on Pico de Orizaba (5675 m a.s.l.), the highest mountain of Mexico, where no numerical dating technique has been applied so far. Lichenometry and dendrochronology allow us to esti- mate minimum ages for both lava flows providing chronological constraints complementary to the ^{36}Cl CRE ages. Therefore, we think that the combination of these three methods could be an alternative ap- proach to date Late Holocene landforms.

2. Study area and previous work at Pico de Orizaba

Pico de Orizaba (19.06° N/−97.25° W; 5675 m a.s.l.) or Citlaltépetl ("mountain of the star" in the

Náhuatl language) is an ice-capped stratovolcano in the eastern part of the Pliocene-Quaternary Trans- Mexican Volcanic Belt (Fig. 1). This chain, associated with the sub- duction of the Cocos Plate beneath the North American Plate, presents a wide variety of volcanic features such as stratovolcanoes (some of them active, e.g. Popocatépetl and Colima), monogenetic cones, dome complexes, maars and calderas.

Carrasco-Núñez (2000) established a chronology of the eruptions of Pico de Orizaba based on K/Ar dating. According to these studies, the construction of Pico de Orizaba began ~0.65 Ma ago, when a large stratovolcano known as Torrecillas covered folded and faulted Cretaceous sedimentary rocks. This first volcanic stage finished with the collapse of Torrecillas cone between ~0.29 and ~0.21 Ma ago, fol- lowed by the formation of a caldera and of a large debris avalanche. A second stage, starting ~0.21 Ma ago, involved the formation of the Espolón de Oro cone as well as the genesis of peripheral dacitic domes. The "Espolón de Oro" cone collapsed ~20 ka ago, producing another massive debris avalanche.

The last volcanic stage began ~20 ka ago with the construction of the modern Citlaltépetl cone and peripheral dacitic domes. Dacitic and high-silica andesitic lava flows basically built the Citlaltépetl cone, an edifice rising to 5675 m a.s.l. Two Plinian eruptions have been reported during the late Pleistocene and Holocene: the first occurred ~13 ka ago and the second 9.0–8.5 ka ago (radiocarbon dating) (Carrasco-Núñez and Rose, 1995; Carrasco-Núñez, 2000; Rossotti and Carrasco-Núñez, 2004). This second event affected all the flanks of the volcano and produced a thick pyroclastic deposit known as the Citlaltépetl ignimbrite. Moreover, the glacier located on the top of the volcano experi- enced several advances during the Late Pleistocene and early Holocene (Vázquez-Selem and Heine, 2011) but most of the associated glacio- geomorphic features are covered by the Citlaltépetl ignimbrite and lava flows and pyroclastic layers emitted during the Late Holocene.
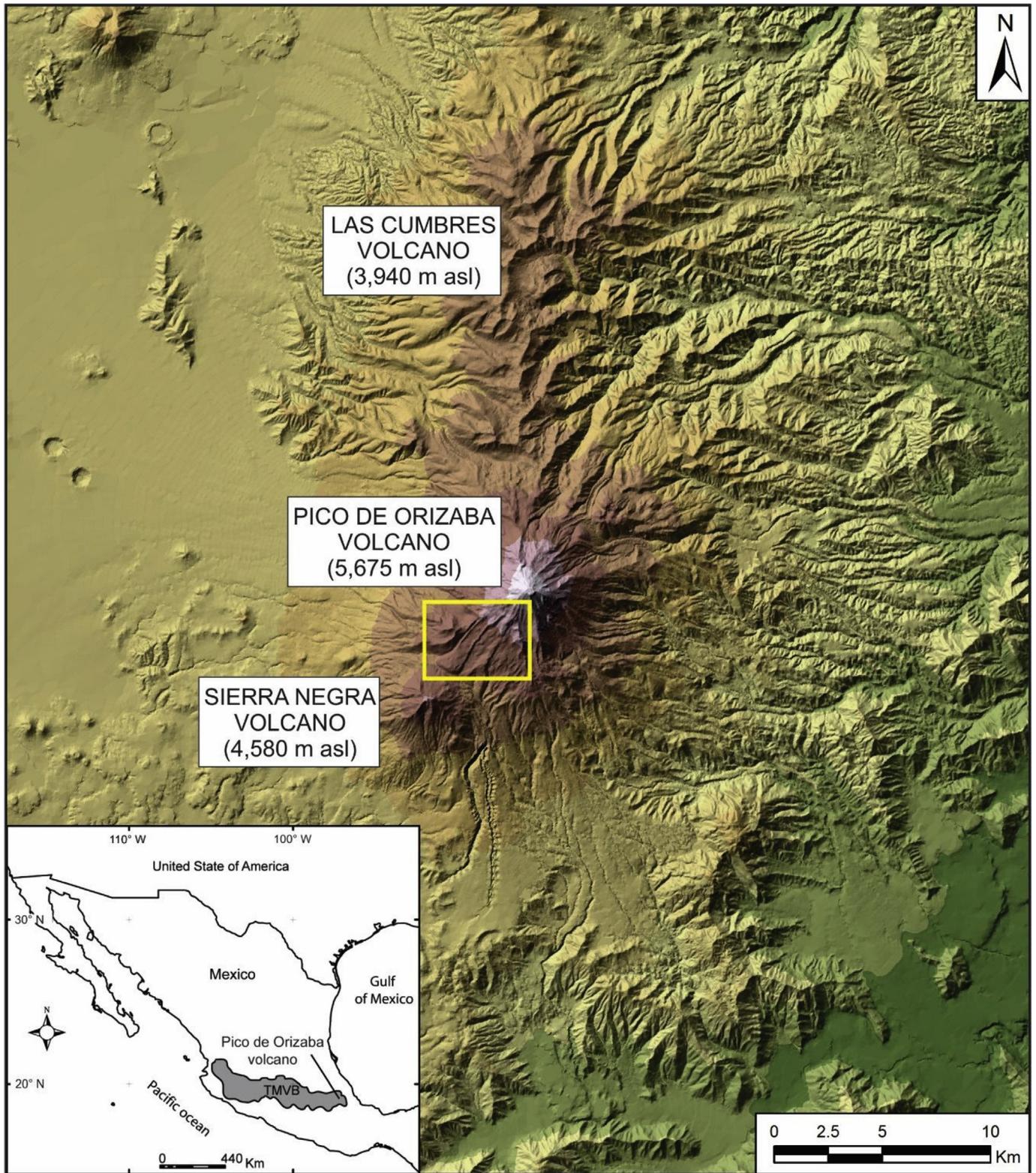
Fig. 1. Location of the study area. Pico de Orizaba, the highest stratovolcano of Mexico, is situated in the eastern part of the Trans-Mexican volcanic belt (TMVB).

Another significant explosive event took place 4.1–4.0 ka ago (radiocarbon dating) on the western flank of the volcano. Due to the eruption of dacitic lavas, blocks, ash flows and lahars were produced at the summit crater and channelized by a glacial cirque into a valley (Siebe et al., 1993). Other Holocene volcanic events occurred at 7020–6200 ka, 3450–3400 ka (The *Jacal* volcanic episode) and 1910–1860 years BP (Texmola volcanic episode) (radiocarbon dating) (Höskuldsson and Robin, 1993).

Although volcanic activity has not been reported over the last years, Pico de Orizaba is still an active volcano. Several lava flows have been assigned to Holocene eruptions, including historical activity such as the one known as the Excola eruptive episode (~1300–1687 AD) (Höskuldsson and Robin, 1993; Carrasco-Núñez, 1997). On the basis of the morphology and structure of these lava flows, Carrasco-Núñez (1997) defined and mapped four categories: (i) single, channeled flows with well-defined lateral levees; (ii) single, blocky flows with lateral levees, rugged top surfaces and steep fronts; (iii) multiple blocky lava flows that sometimes exhibit lateral levees; (iv) massive lava flow fields, including single and multiple flows that present lateral levees and blocky surfaces. The two lava flows dated in this work, informally named here "A" and "B" (Fig. 2), belong to the second group described above. Both moved from the crater to the southwest of the modern cone. They are porphyritic dacites, showing a variation in silica content from 60 to 66 wt%, and their volumes have been estimated at 130×10^6 m^3 for lava flow "A" and 38×10^6 m^3 for lava flow "B" (Carrasco-Núñez, 1997). Based on their distribution, morphology and stratigraphic relationships, Carrasco-Núñez (1997) suggested that lava flow "A" possibly corresponded to one of the three historically con- firmed eruptions during the 16th century (1537; 1545 or 1566 AD), and lava flow "B" corresponded to the eruption of 1613 AD. Similarly, Höskuldsson and Robin (1993) tentatively ascribed lava flow "A" to the eruption of 1545 AD, and lava flow "B" to that of 1613 AD. The three methods used in this study should allow validating or disproving these assignations.

The climate of the study area, located at altitudes between 4000 and 4500 m a.s.l, is characterized by relatively cold temperatures and moderate precipitations. According to Lauer (1978), temperatures do not change significantly during the year; the mean annual temperature being ~ 5 °C at 4000 m a.s.l and 0 °C at 5000 m a.s.l. The mean number of days with frost is 200 and 360, respectively. Mean annual pre- cipitation ranges from ~900 (4000 m a.s.l) to ~800 mm (5000 m a.s.l), with most of it occurring during the wet season (May–October) and during some weeks in winter associated with cold fronts coming from higher latitudes. The vegetation is mainly *Pinus hartwegii* tree stands, the timberline being at ~4000 m a.s.l, and tufted grass associations of *Calamagrostis tolucensis*, *Festuca tolucensis* and *Muehlenbergia quadridenta* from ~4000 to ~4400 m a.s.l.

The front and lateral walls of the lava flow "A", at 4000 m a.s.l, are covered by *Pinus hartwegii* tree stands. They become sparser on the top surface of the lava flow with isolated individuals reaching 4300 m a.s.l. Lava flow "A" is also colonized by individuals of the alpine woody shrub *Juniperus monticola*, a *krummholz* species that can grow at ele- vations up to ~4500 m a.s.l. This woody shrub has been considered as a species with high dendrochronological potential, because of its annual growth rings and a lifetime of hundreds of years (Villanueva-Díaz et al., 2016). In contrast, lava flow "B" (front at 4450 m a.s.l) lacks these woody species since the altitude is higher. However, the rock surfaces of both lava flows are widely colonized by various lichen species in- cluding *Rhizocarpon geographicum*.
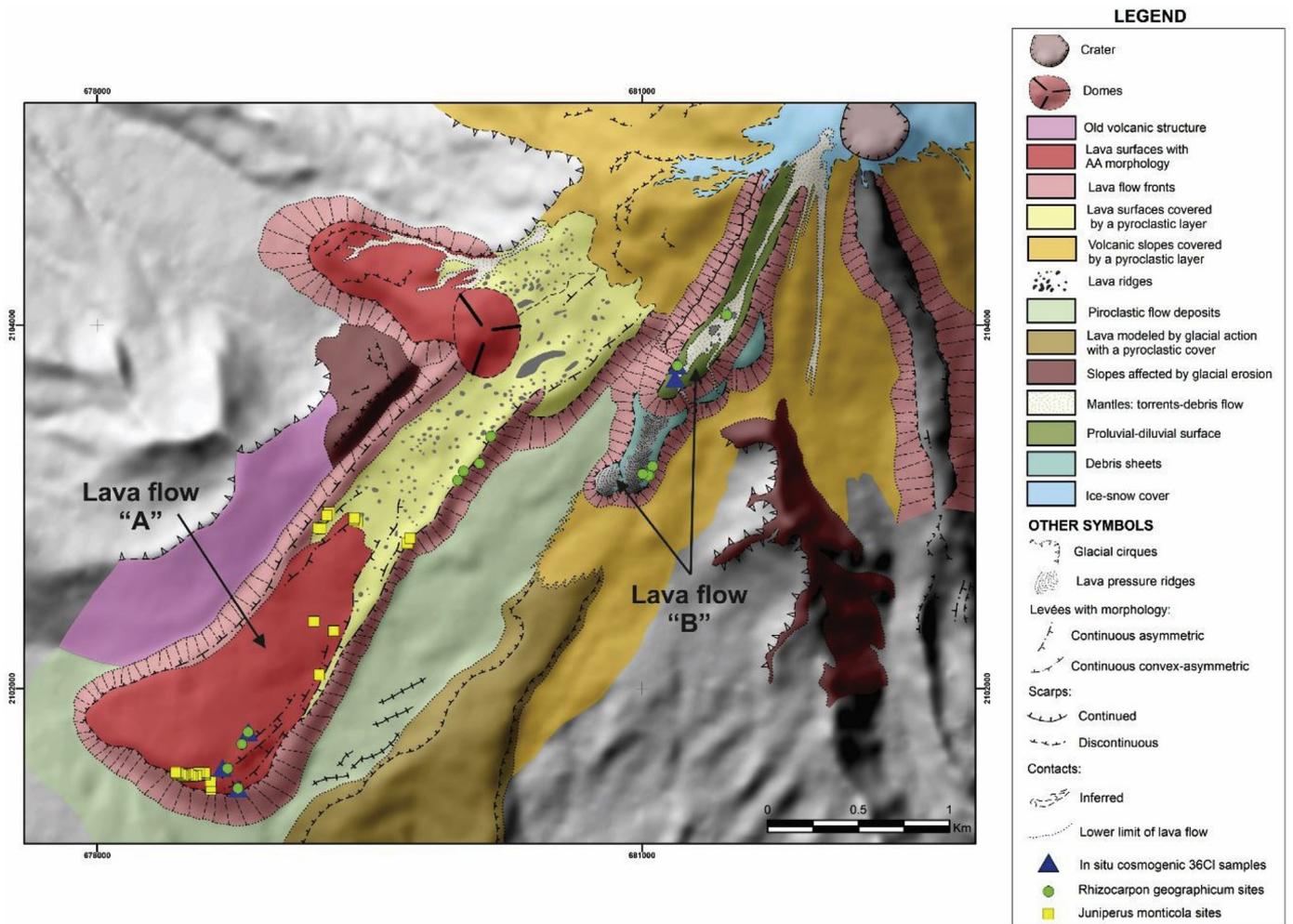
Fig. 2. Geomorphological map from the southwestern slope of Pico de Orizaba. The location of the samples collected for *in situ*-produced ^{36}Cl CRE dating, liche- nometry ("*Rhizocarpon geographicum* sites") and dendrochronology (*Juniperus monticola* sites) on both lava flows is shown.

3. Materials and methods

3.1. Geomorphological mapping

A detailed geomorphological map (scale 1: 10,000) of the south- western flank of Pico de Orizaba volcano was produced from the ana- lysis of vertical aerial photographs (scale 1:60,000, Instituto Nacional de Estadística y Geografía de México, INEGI). To represent the land- forms in detail, the standard procedures proposed by Bashenina (1977) and Simonov (1972) were used and adapted to the characteristics of the study area. These mapping methods classify the relief based on mor- phogenetical and morphochronological criteria that include data of li- thology and morphostructures using several colours and areal, lineal and points symbols. The map was verified with fieldwork and then it was digitized using ArcMap 10.2.2 software.

3.2. In situ-produced ^{36}Cl CRE dating

3.2.1. Sampling strategy and analytical methods

To determine the ^{36}Cl CRE ages of the lava flows, five samples were collected with hammer and chisel from the uppermost ~5 cm of solid rock surfaces (Fig. 2). Three of them (Pico 4, 5 and 6) were taken from lava flow A. Pico 4 was collected from the surface of a > 1 m high, stable boulder on a levee on the left margin of the lava flow, whereas Pico 5 and Pico 6 came from the surfaces of tumuli features situated on the top of the lava flow (Fig. 3). The other two samples (Pico 7 and Pico 8) were collected from the surfaces of prominent tumuli located on the surface of lava flow B (Fig. 4). The field data and sample characteristics of the five samples are given in Table 1. All sampled surfaces were well preserved, showing no signs of erosion, weathering or boulder toppling. Therefore, potential bias in the ^{36}Cl surface concentrations induced by these post-cooling geomorphological processes are minimized. More- over, the protruding geometries of the sampled features reduce the risk of surface shielding by snow, tephra fall associated with volcanic ac- tivity of Pico de Orizaba, and soils.

Lichens, mosses and other organic matter were removed from the samples with a brush. Then, whole rock samples were crushed with a roller grinder and sieved to retrieve the grain size fraction (0.25–0.50 mm) at Instituto de Geofísica of the Universidad Nacional Autónoma de México (UNAM). The chemical preparation was carried out at the Centre Européen de Recherche et d'Enseignement des Géosciences de l'Environnement (CEREGE; France). Aliquots of the bulk rock were taken for the analyses of the major and trace element con- centrations at Activation Laboratories (Ancaster, Canada) (Table 2), needed to compute the low-energy neutron flux in the samples, which induces the ^{36}Cl production from capture of the low-energy neutrons on ^{35}Cl. These bulk rock analyses also allowed us to confirm the dacitic composition of the rock samples (see section 2); i.e. SiO_2 concentrations of ~64% and $Na_2O + K_2O$ concentrations of ~6.5% correspond to a dacite according to the "total alkalies versus silica" classification by Le Bas et al. (1986).

About 80 g of the sample grains were washed in ultrapure water to remove fine-grained powder and then leached in a dilute HF/HNO_3 mixture to dissolve ~15–20% of the initial sample mass to remove atmospheric ^{36}Cl and reduce the potentially Cl-rich groundmass (Schimmelpfennig et al., 2009). Then, these etched samples were dried and 2 g aliquots of each sample were taken for analysis of the major elements at the Activation Laboratories (Ancaster, Canada) (Table 3), because Ca, K, Ti and Fe are the target elements for ^{36}Cl production by spallation (Ca, K, Ti, Fe) and muon capture (Ca, K). Before total sample dissolution of the remaining sample material (~60 g) in a dilute HF/HNO_3 mixture, a ^{35}Cl-enriched spike (~99%) was added to each sample and to one chemistry blank for isotope dilution (Ivy-Ochs et al., 2004). The subsequent steps of AgCl

precipitations and removal of sulfur were performed according to the methods described in Schimmelpfennig et al. (2011). Both the $^{36}Cl/^{35}Cl$ and $^{35}Cl/^{37}Cl$ ratios, measured in the year 2015 by AMS isotope dilution at the French national AMS facility (CEREGE, France) (Arnold et al., 2013), were normalized to standard KNSTD1600 (Sharma et al., 1990) with an assigned $^{36}Cl/^{35}Cl$ ratio of $(2.112 \pm 0.905) \times 10^{-12}$, and assuming a natural ratio of 3.127 for the $^{35}Cl/^{37}Cl$ ratio. From these ratios, the ^{36}Cl and Cl concentrations were calculated. The analytical data are presented in Table 4.

3.2.2. ^{36}Cl CRE age calculations

We calculated the ^{36}Cl CRE ages according to the formalism pro- posed by Schimmelpfennig (2009) and Schimmelpfennig et al. (2009). The results shown in Table 4 and discussed below are based on the following ^{36}Cl production rates and parameters, referenced to sea level and high latitude, using the time-invariant "St" scaling (Stone, 2000):

42.2 ± 4.8 atoms ^{36}Cl (g Ca)$^{-1}$ yr^{-1} for spallation of Ca (Schimmelpfennig et al., 2011), 148.1 ± 7.8 atoms ^{36}Cl (g K)$^{-1}$ yr^{-1} for spallation of K (Schimmelpfennig et al., 2014), 13 ± 3 atoms ^{36}Cl (g Ti)$^{-1}$ yr^{-1} for spallation of Ti (Fink et al., 2000), 1.9 ± 0.2 atoms ^{36}Cl (g Fe)$^{-1}$ yr^{-1} for spallation of Fe (Stone et al., 2005), and 696 ± 185 neutrons (g air)$^{-1}$ yr^{-1} at the Earth's surface/atmosphere interface for the production rate of epithermal neutrons from fast neutrons in the atmosphere (Marrero et al., 2016). Applying the ^{36}Cl production rates from Ca and K spallation calibrated by Marrero et al. (2016) of 52.2 ± 5.2 atoms ^{36}Cl (g Ca)$^{-1}$ yr^{-1} and 150 ± 15 atoms ^{36}Cl (g K)$^{-1}$ yr^{-1}, respectively, yields ^{36}Cl CRE ages that are insignificantly younger (< 3%).
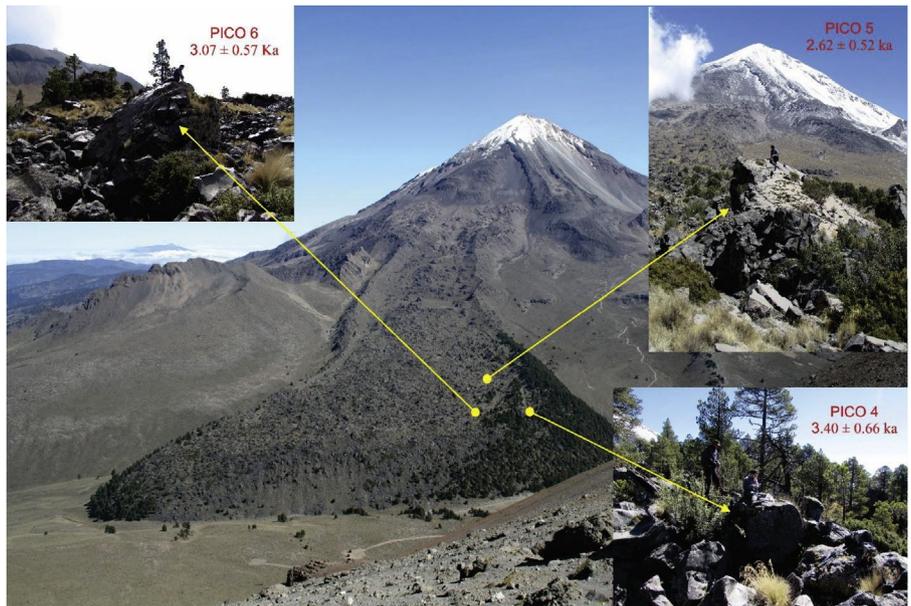

Fig. 3. Locations, photographs and ^{36}Cl CRE ages of the geomorphic features sampled for *in situ*-produced ^{36}Cl CRE dating on lava flow "A".
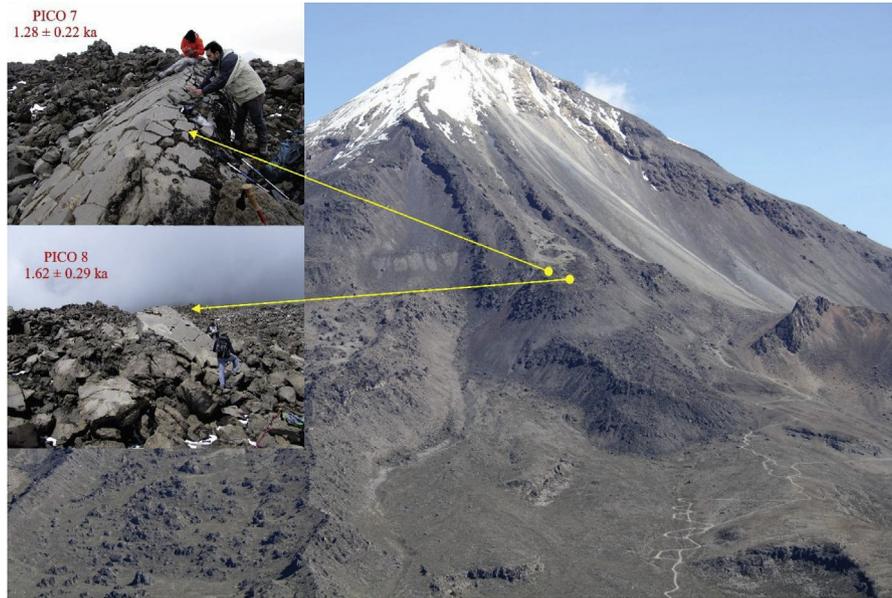
Fig. 4. Locations, photographs and [36]Cl CRE ages of the geomorphic features sampled for *in situ*-produced [36]Cl CRE dating on lava flow "B".

Table 1
Field data and sample characteristics of [36]Cl dated samples from lava flows of Pico de Orizaba. The shielding factor was calculated using the Topographic Shielding Calculator v1.0 provided by CRONUS-Earth Project (2014).

Sample	Latitude	Longitude	Altitude (m.a.s.l)	Thickness (cm)	Shielding factor
Pico 4	18.99	−97.30	4144	1.5	0.9945
Pico 5	19.00	−97.30	4165	1.5	0.995
Pico 6	18.99	−97.30	4166	3.0	0.9968
Pico 7	19.01	−97.27	4831	4.0	0.9931
Pico 8	19.01	−97.28	4815	2.0	0.9782

Table 2
Major and trace element concentrations in bulk rock samples from lava flows of Pico de Orizaba, before chemical treatment (see text). Analyses done at Activation Laboratories (Ancaster, Canada).

Sample	SiO_2 (wt-%)	Na_2O (wt-%)	MgO (wt-%)	Al_2O_3 (wt-%)	MnO (wt-%)	H_2O (wt-%)	Sm (ppm)	Gd (ppm)	K_2O (wt-%)	CaO (wt-%)	Cl (ppm)	TiO_2 (wt-%)	Fe_2O_3 (wt-%)	P_2O_5 (wt-%)	U (ppm)	Th (ppm)	Li (ppm)
Pico 4	64.26	4.22	2.38	15.58	0.08	0.5	4.3	3.2	2.34	4.41	500	0.611	5.25	0.16	2.6	7.6	14
Pico 5	63.95	4.12	2.18	15.39	0.08	0.5	4.4	3.4	2.28	4.39	500	0.587	4.95	0.16	2.5	7.2	15
Pico 6	64.47	4.23	2.26	15.77	0.08	0.5	4.2	3.4	2.39	4.32	600	0.614	5.22	0.17	2.6	7.3	15
Pico 7	63.95	4.07	2.75	15.26	0.08	0.5	4.3	3.5	2.13	4.62	700	0.651	5.38	0.17	2.0	5.5	14
Pico 8	63.94	4.05	2.72	15.15	0.08	0.5	4.6	3.6	2.18	4.38	400	0.644	5.26	0.19	2.2	5.9	14

Table 3
Concentrations of the [36]Cl target elements, measured in splits taken from the samples after the chemical pre-treatment (see text). Analyses done at Activation Laboratories (Ancaster, Canada).

Sample	CaO %	K2O %	TiO2%	Fe2O3%
Pico 4	3.92	2.56	0.71	4.93
Pico 5	3.74	2.59	0.62	4.65
Pico 6	3.73	2.66	0.64	4.83
Pico 7	4.72	2.63	0.74	5.74
Pico 8	3.78	2.44	0.71	5.24

The nucleogenic and muonic scaling factors were calculated ac- cording to the time-invariant scaling model of Stone (2000), using CosmoCalc (Vermeesch, 2007), and applying the atmosphere standard model (N.O.A.A, 1976). When we apply the same scaling method but implementing a correction for the time-variant paleomagnetic field intensity, following the so-called "Lm" scaling approach in Balco et al. (2008), the resulting [36]Cl ages are older by 5–7%. Moreover, the use of the local atmospheric pressure according to the ERA-40 model (Uppala et al., 2005) or inferred from the closest weather station (Loma Grande; 18.92 N, −97.23 W, 2722 m a.s.l.) instead of the standard atmosphere pressure, together with the time-variant Lm scaling approach, yields [36]Cl ages older by 14–15% compared to the time-invariant Stone (2000) scaling. A high-energy attenuation length of 160 g cm^{-2} was applied. The shielding factors were calculated with the Topographic Shielding Calculator v1.0 provided by CRONUS-Earth Project (2014). A density of 2.5 g/cm^3 is assumed for all samples. Using a lower or higher density values (2.3–2.8 g/cm^3), the results would change by less than 1%. Considering the good state of preservation of the sampled surfaces, no corrections for erosion were applied. Similarly, considering that today the snow pack usually remains only a few days during winter, the influence of the snow cover on the production rates when integrated over the last thousands of years is assumed to be insignificant (see further discussion in section 5). The 1σ uncertainties associated with the [36]Cl CRE ages (Table 4) were calculated through full propagation of analytical and production rate errors.

Table 4

Analytical ^{36}Cl data and resulting ^{36}Cl CRE ages for samples from lava flows of Pico de Orizaba. Age uncertainties (1σ) include production rate errors as well as analytical errors; numbers in parenthesis correspond to analytical errors only.

Sample	Sample weight (g)	Mass Cl (mg) added by spike	$^{35}Cl/^{37}Cl$	$^{36}Cl/^{35}Cl$ (10^{14})	Cl (ppm)	^{36}Cl conc $(10^3$ atoms g$^{-1})$	^{36}Cl CRE age (ka)
Pico 4	65.17	1.958	3.442 ± 0.016	9.11 ± 0.50	397 ± 28	511 ± 43	3.40 ± 0.66 (0.34)
Pico 5	64.19	1.964	3.456 ± 0.019	7.35 ± 0.40	387 ± 30	403 ± 36	2.62 ± 0.52 (0.27)
Pico 6	68.28	1.965	3.456 ± 0.010	8.83 ± 0.43	364 ± 21	456 ± 32	3.07 ± 0.57 (0.27)
Pico 7	66.92	1.963	3.613 ± 0.018	5.63 ± 0.35	251 ± 15	209 ± 17	1.28 ± 0.22 (0.13)
Pico 8	66.00	1.952	3.612 ± 0.019	6.49 ± 0.43	254 ± 16	243 ± 21	1.62 ± 0.29 (0.17)
Blank	–	1.956	377.4 ± 9.4	0.348 ± 0.078	–	–	–

3.3. Dendrochronology

3.3.1. Field sampling

In order to estimate the minimum age of lava flow "A" based on tree-ring counting, cross-sections from 32 individuals of the alpine woody shrub *Juniperus monticola* f. *orizabensis* Martínez from the side and top slopes of this lava flow, between 4140 and 4515 m a.s.l. (Fig. 2), were collected. Samples were taken by the use of a chain saw to cut across the main stem of dead specimens plants (n = 27) or a major branch of living but old-looking specimens (n = 5) (Fig. 5), pre- ferentially targeting cylindrical, symmetrical segments without growth disturbances. Due to the irregular growth pattern of rings, with nu- merous missing rings depending on the side of the trunk observed, samples from cores on living individuals were considered of limited use for dating purposes and therefore were not collected. The location of each sampled specimen was recorded in a GPS with a precision of ± 3 m. Although *Pinus hartwegii* trees also grow on lava flow "A", they were not used for dating purposes as preliminary sampling showed that they are younger than 250 years.

3.3.2. Laboratory analysis

All samples were sanded with a belt sander with progressively finer sandpaper from 50 grits (125–149 μm) to 400 grit (20.6–23.6 μm) (Stokes and Smiley, 1968). Once the annual rings were clearly visible, growth rings were counted from the pit to the bark under the microscope at 40X magnification. Counts were performed along two per- pendicular lines on each cross section in order to compare and crossdate the dendrochronological series. Then, the growth rings were measured with a VELMEX measuring device (Robinson and Evans, 1980) at 0.001 mm resolution. We used the software COFECHA (Grissino-Mayer, 2001) to identify possible dating problems such as missing or false rings and to determine the dating quality.

3.4. Lichenometry

In this work, we used lichenometry on condition that the following criteria are met: (i) a volcano, although active, must not have had re- cent explosive activity (i.e. pyroclastic flows) that could have affected the lichen growth; (ii) under favorable environmental conditions, sur- faces of thousands of years can be dated by measuring the growth of lichens such as *Rhizocarpon geographicum*, a species that can colonize volcanic rocks on tropical mountains; and (iii) as lichenometry usually provides minimum ages, it should be combined with other dating methods.

Although lichenometry is a simple method, there is no agreement about how the thalli should be measured. For the lichen measurements in this work, we selected several sites close to the samples collected for ^{36}Cl CRE dating and dendrochronology. We chose protruding features with smooth surfaces that were not fragmented or affected by volcanic or erosive processes after
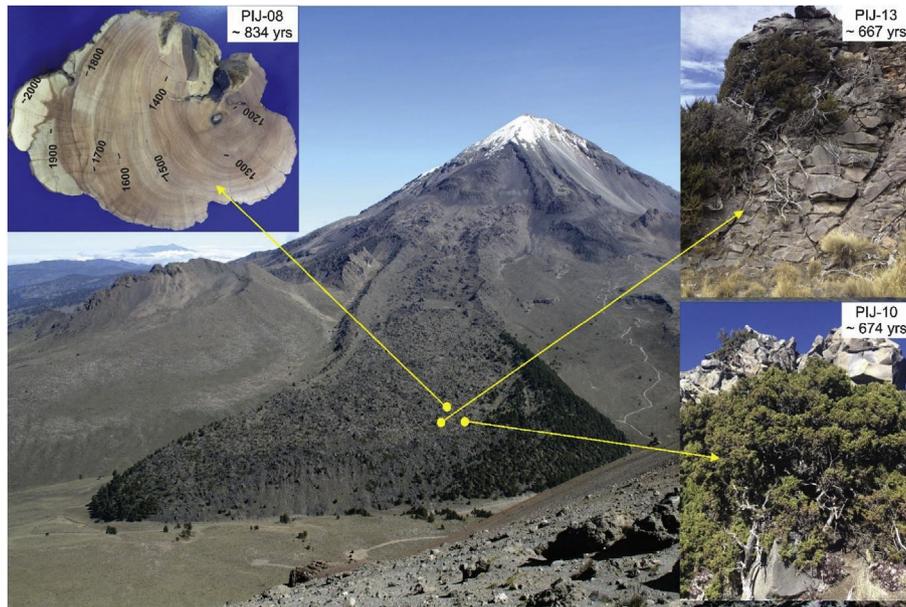
Fig. 5. Locations, characteristics and ages of the biggest individuals of *Juniperus monticola* f. *orizabensis* Martínez that grow on lava flow "A". One of them is older than 800 years and several individuals appear dead due to fires that affected the lowest area of the lava flow.

Table 5

Dendrochronology-based ages of sampled individuals of *Juniperus monticola f. Orizabensis Martínez* growing on lava flow A. The lines highlighted in green correspond to the oldest specimens recorded. Sampling took place in March 2015.

Sample	Latitude	Longitude	Altitude (m. a.s.l)	Innermost tree-ring (AD year)	Outermost tree-ring (AD year)	Age (years)	Status
PIJ-01	18.99	-97.30	4143	1796	2014	218	Live
PIJ-02	18.99	-97.30	4145	1643	2014	371	Live
PIJ-03	18.99	-97.30	4147	1674	2014	340	Live
PIJ-04	18.99	-97.30	4144	1582	1999	417	Death
PIJ-05	18.99	-97.30	4144	1800	1992	192	Death
PIJ-06	18.99	-97.30	4144	-	-	322	Death
PIJ-07	18.99	-97.30	4147	-	-	304	Death
PIJ-08	18.99	-97.30	4140	1178	2012	834	Death
PIJ-09	18.99	-97.30	4150	1617	2009	392	Death
PIJ-10	18.99	-97.30	4145	1325	1999	674	Death
PIJ-11	18.99	-97.30	4157	1680	2009	329	Death
PIJ-12	18.99	-97.30	4152	1619	2014	395	Live
PIJ-13	18.99	-97.30	4149	1332	1999	667	Death
PIJ-14	18.99	-97.30	4149	-	-	214	Death
PIJ-15	18.99	-97.30	4154	1364	2000	636	Death
PIJ-16	18.99	-97.30	4155	1527	1876	349	Death
PIJ-17	18.99	-97.30	4153	1520	2004	484	Death
PIJ-18	18.99	-97.30	4156	1672	2004	332	Death
PIJ-19	18.99	-97.30	4153	1600	2000	400	Death
PIJ-20	18.99	-97.30	4145	1390	1999	609	Death
PIJ-21	19.00	-97.29	4226	-	-	243	Death
PIJ-22	19.00	-97.29	4217	-	-	306	Death
PIJ-23	19.00	-97.29	4337	1418	2014	596	Live
PIJ-24	19.01	-97.29	4326	1740	2000	260	Death
PIJ-25	19.01	-97.29	4268	1487	2000	513	Death
PIJ-26	19.01	-97.29	4263	1700	1999	299	Death
PIJ-27	19.01	-97.29	4270	1896	2008	112	Death
PIJ-28	19.01	-97.29	4268	-	-	230	Death
PIJ-29	19.01	-97.29	4267	-	-	261	Death
PIJ-30	19.01	-97.29	4259	1745	1999	254	Death
PIJ-31	19.01	-97.29	4242	1716	2000	284	Death
PIJ-32	19.00	-97.29	4246	-	-	254	Death

cooling. At each measurement site, the largest diameter of the at least 5 biggest circular thalli of *Rhizocarpon geo- graphicum* were measured with a Bernier calibrator. Digital photographs parallel to the surface of the lichen were taken, using a scale (one peso coin of 21 mm of diameter). Because the dated features are lava flows, there is no possibility of inheritance of thalli as may occur on sedi- mentary deposits. This criterion has usually been applied in volcanic environments and has been validated by the analysis of artificial sur- faces with a known age (Burbank, 1981; Porter, 1981; O'Neal, and Schoenenberger, 2003; O'Neal et al., 2013).

To determine the age of the largest lichen at each point, we used a growth rate of 0.23 mm a^{-1} for *Rhizocarpon geographicum* established by Palacios et al. (2012) on Iztaccíhuatl volcano, 150 km to the west of Pico de Orizaba and at an altitude similar to that of the present study area. Detailed fieldwork analyzing lichens on deglaciated surfaces of known age by photogrammetry was conducted at the Pico de Orizaba. It confirmed the growth rate obtained at the Iztaccíhuatl volcano. We do not use the significantly higher (0.6 mm a^{-1}) growth rate of *Rhizo- carpon geographicum* reported from the Volcán Barú, Panamá (Zotz, 2017), since they were derived from sites at lower elevation (3350–3450 m a.s.l) and with higher precipitation.

4. Results

4.1. Geomorphological map

The geomorphological map (Fig. 2) show that the upper part of the Lava flow "A" is covered by a pyroclastic layer, indicating explosive activity likely associated with the growth and destruction of domes sometime after its emission. Moreover, most of the surface of the lava flow "A" is formed by tumuli features and its edge has levees and steep lava fronts. Regarding Lava flow "B", it is formed by two superimposed flows. Due to their similar size, morphology (well-preserved blocky flows with lateral levees, rugged top surfaces and steep fronts) and thickness, they likely were emitted during the same volcanic event. Both flows are partially covered by proluvial-diluvial surfaces, debris flows and debris sheets. Around Lava flows "A" and "B, old volcanic structures, volcanic slopes covered by a pyroclastic layer, pyroclastic flow deposits and slopes affected by glacial erosion were identified.

4.2. In situ-produced ^{36}Cl CRE dating

The ^{36}Cl CRE ages of the southwestern lava flows of Pico de Orizaba are shown in Table 4. The three CRE ages from the lava flow "A" range from 3.40 ± 0.66 ka to 2.62 ± 0.52 ka, whereas the two samples from the lava flow "B" lead to CRE ages of 1.28 ± 0.22 ka and 1.62 ± 0.29 ka. The 17–20% uncertainty associated with the ^{36}Cl CRE ages result from the high natural chlorine concentration of 250–400 ppm in the lava flow samples. It implies a ^{36}Cl contribution of ~61–71% from a Cl- related ^{36}Cl production reaction, i.e. the capture of low-energy (i.e. thermal and epithermal) neutrons of cosmogenic origin on ^{35}Cl (Phillips et al., 2001). Due to the complexity of this production reaction and its dependency on various sample-specific environmental and surface-re- lated factors (e.g. snow cover, surface geometry; Zreda et al., 1993; Masarik et al., 2007; Dunai et al., 2014, section 5), which are difficult to accurately estimate, we assigned a conservative 30% uncertainty to the ^{36}Cl contribution from this production reaction pathway (Schimmelpfennig et al., 2009). The ^{36}Cl contribution from capture of non-cosmogenic low-energy neutrons (i.e. those related to the α-decay of the local U-Th) on ^{35}Cl is insignificant due to the young age of these igneous rocks; it is estimated to < 0.2% of the total ^{36}Cl production. The contribution from the better understood ^{36}Cl production from spallation of Ca, K, Fe and Ti amounts to ~28–37% of the total ^{36}Cl production. In particular, the ^{36}Cl contribution from spallation of Ca of only 7–11% explains why the choice of the ^{36}Cl production rate from spallation of Ca does not significantly affect the calculated ^{36}Cl CRE ages (see section 3.1.2.). The ^{36}Cl contribution from the capture of slow negative muons is estimated to less than 1%.

Considering their associated analytical uncertainties (Table 4), the three ^{36}Cl CRE ages from lava flow "A" and the two ages from lava flow "B" are not significantly different, respectively, as verified by the χ^2 test proposed in Ward and Wilson (1978), considering the 95% confidence interval (2σ). This allows us to calculate arithmetic ^{36}Cl CRE mean age of 3.03 ± 0.70 ka for flow A and 1.45 ± 0.35 ka for flow B (Table 7). The uncertainties associated with these ^{36}Cl CRE mean ages include the standard deviations as well as the analytical and production rate errors quadratically propagated. Calculating mean ages that are weighted by their inverse variances (1/σ^2), considering the full (i.e. analytical and production rate) errors in the individual ages, results in ages that are similar to the arithmetic means: 2.97 ± 0.33 ka for flow A and
1.40 ± 0.18 ka for flow B.

4.3. Dendrochronology

The ages of 32 specimens of *Juniperus monticola* from lava flow "A" ranged from 112 to 834 years (Figs. 5 and 8 and Table 5); six specimens were older than 600 years (PIJ-08; PIJ-10; PIJ-13; PIJ-15; PIJ-20). The precise date of the youngest ring of death specimens was determined by comparing their growth patterns with those of living specimens. The oldest specimen (PIJ-08) comes from 4140 m a.s.l., has 834 growth rings and lived from 1178 CE (innermost ring) to 2012 CE (outermost ring). The youngest one (PIJ-27), with 112 growth rings, grew from 1898 CE to 2008 CE at 4270 m a.s.l. Sampling took place in March 2015, whereby the outermost ring of living specimens is from 2014 CE. The outermost ring of 41% of the dead specimens formed in 1999 CE and 2000 CE, probably as a result of extensive fires recorded in 1998 in connection with a strong El Niño event. On the basis of the age of the oldest sample, we conclude that lava flow "A" was already in place by 1178 CE.

4.4. Lichenometry

At the front of lava flow "A", between 4140 and 4170 m a.s.l., 4 measurement sites (Sites-1, 2, 3 and 4) close to the tree stands of *Pinus hartwegii* were established (Fig. 2). A high biodiversity of lichens and bryophytes showing a strong competition between them was observed   at the lower sites (Site 1 and 2). However, this competition significantly decreased towards the higher sites (Sites 3 and 4) where thalli of *Rhi- zocarpon geographicum* grow extensively. At sites 3 and 4, thalli of *Rhizocarpon geographicum* with ages ranging between 185 and 720 years were found. By contrast, the most external and highest sites (Sites-11, 12, 13 and 14), on the left levee of lava flow "A" at 4400–4500 m a.s.l., present colonies formed by several long-lived individuals whose ages may reach 1000 years. The oldest thallus lead to an age of 1130 years (Figs. 6 and 8 and Table 6).

Lichens were measured at 6 sites along lava flow "B". Two of them (Sites 5 and 6) are located between 5000 and 4800 m a.s.l., where the lava flow starts, and the four others (Sites 7, 8, 9 and 10) are located between at 4590–4570 m a.s.l., close to the front. The two higher sites (Sites 5 and 6) only present small lichens with a maximum age of 400 years due to the presence of a pumice sheet, which partially covers the lava flow, and to a remarkable competition with bryophytes. At lower altitudes, i.e. at Sites 7, 8, 9 and 10, the lichens are more abundant. There, the ages of the biggest thalli, found on well-exposed surfaces (where competition with other species decreases), exceed 1000 years. The largest thallus lead to an age of 1090 years (Figs. 7 and 8 and Table 6).

5. Discussion

The arithmetic ^{36}Cl CRE mean age of 3.03 ± 0.70 ka calculated from the three lava flow "A" samples is ~2 ka older than the minimum ages provided by the oldest thalli of *Rhizocarpon geographicum* (~1.13 ka) and by the tree rings of *Juniperus monticola* (~0.834 ka) (Table 7). This difference indicates that the oldest individuals of *Rhizocarpon geographicum* and *Juniperus monticola* most probably do not correspond to the first colonization phase of both species. This may be due to the impact of fires, the volcanic activity or the natural mortality in a pio- neering community (Loso and Doak, 2006). Indeed, evidence of recent fires is observed in the lower part of the lava flow where only young specimens of *Rhizocarpon geographicum* are present. On the other hand, the presence of larger thalli in the lowest part of lava flow "A" may be limited due to the competition of *Rhizocarpon geographicum* with other species of lichens or bryophytes related to milder environmental con- ditions at lower elevation compared to those in the upper part of the lava flow. Moreover, a pyroclastic flow deposit partially covers the highest part of the lava flow, indicating explosive activity after the emission of the lava flow. Thus, pyroclastic flows most likely have burned/buried individuals of *Rhizocarpon geographicum and Juniperus monticola* colonizing the highest areas of the lava flow. In contrast, the lateral levees, less affected by the pyroclastic flows, apparently acted as a refuge for both species. However, despite these local constraints in pioneering colonization, the similar ages of the oldest individual of *Rhizocarpon geographicum* and *Juniperus monticola* provide a consistent minimum age supporting the ^{36}Cl CRE mean age. The three performed methods clearly indicate that lava flow "A" was emplaced substantially earlier than the mid-16th century as was previously assumed, based on stratigraphy and correlation with historical records (Höskuldsson and Robin, 1993; Carrasco-Núñez, 1997). The ^{36}Cl CRE ages calculated for the lava flow "B" samples (Pico 7 and 8) lead to an arithmetic mean of 1.45 ± 0.35 ka. This ^{36}Cl CRE mean age cannot be compared with dendrochronology as the lava flow is located above 4500 m a.s.l., an elevation at which *Juniperus monticola* cannot grow. Moreover, thalli of *Rhizocarpon geographicum* are scarce and small due to debris sheets that covered the inner surface of the upper lava flow. However, four well defined and homogeneous thalli larger than 215 mm (~1000 years) were found in the levees of the lower flow (Fig. 7). The morphology, ^{36}Cl CRE ages and lichenometry are similar in both flows and therefore they probably were emitted during the same volcanic event. The ages obtained from both dating methods are consistent within uncertainties, which illustrates their usefulness in dating young landforms. Thus, lava flow "B" was emplaced between ~1800 and ~1000 yr BP that is sev- eral hundred years before the eruptive episode of 1613 CE to which it was associated by Höskuldsson and Robin (1993) and Carrasco-Núñez (1997). Therefore, the lava flow "A" ^{36}Cl CRE mean age of 3.03 ± 0.70 ka suggests that the corresponding eruption might be related to the *Jacal* (3450–3400 yr ago) eruptive episode described for the Pico de Orizaba by Höskuldsson and Robin (1993). Based on the lava flow "B" ^{36}Cl CRE mean age of 1.45 ± 0.35 ka, the corresponding eruption can tentatively be associated with the Texmola (1910–1860 years BP) eruptive episode (Höskuldsson and Robin, 1993). Such as these lava flows are not of the 16th and 17th century eruptions, the lava flows related with these historical volcanic activity could be located on the northern flank of the volcano around the crater. Although the un- certainties associated with the presented data hinder us so far to establish a better-resolved chronology, the combination of ^{36}Cl CRE dating, lichenometry and dendrochronology as performed in this study provides a useful approach to constrain lava flow emplacement ages.
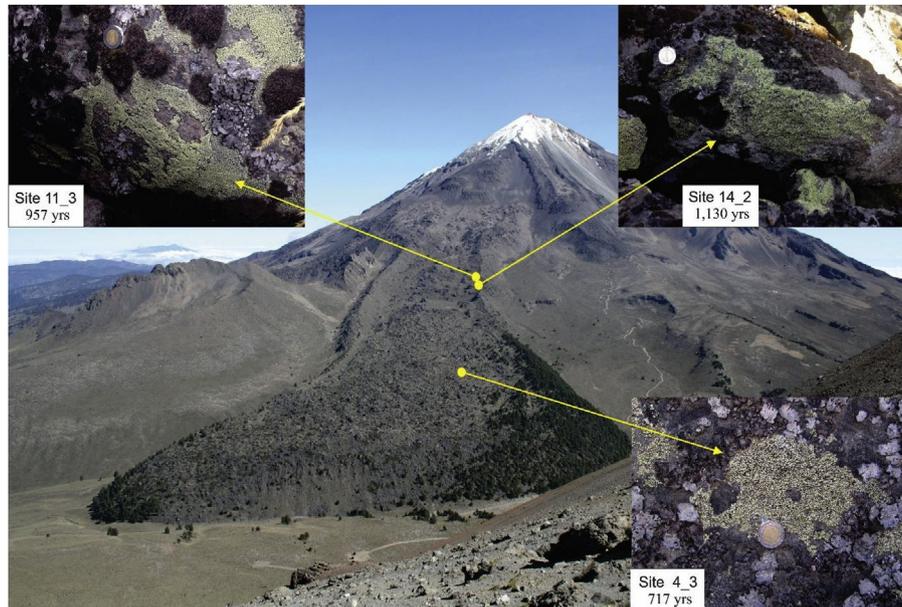
Fig. 6. Locations, characteristics and ages obtained from the biggest lichens found on lava flow "A". The thalli of *Rhizocarpon geographicum* located at the lowest area of the lava flow have a smaller size than the individuals that grow on the upper part of the levees of the lava flow due to the effect of fires.

A possible limitation that could affect the ^{36}Cl CRE ages is related to the high concentrations of ^{35}Cl measured in the five rock samples (section 4.1). The ^{36}Cl accumulation in these samples is therefore significantly affected by the thermal and epithermal neutron flux, which is captured by ^{35}Cl to produce ^{36}Cl. This flux has a high sensitivity 1) to the concentration of hydrogen (snow cover or pore water in the rock or soil surface) in the environment and it is still investigated how to correctly model the effect of hydrogen on the different cosmo- genic nuclide production reactions of ^{36}Cl (Masarik et al., 2007; Zweck et al., 2013; Dunai et al., 2014; Delunel et al., 2014) and 2) to the geometry of the rock surface (Zreda et al., 1993) (section 4.1). Today, the presence of water and snow in Pico de Orizaba mainly occurs during the wet season (May–October) and during some weeks in winter, when cold fronts from higher latitudes reach the study area. During episodes of different climate conditions over the last millennia, such as the Little Ice Age, the annual snow cover might have differed from today. How- ever, it has been shown based on paleo-lake records (Rodriguez- Ramírez et al., 2015) that the Little Ice Age in Mexico was characterized by several long dry intervals (~100–150 years) rather than by cold and wet conditions. Therefore, the effect of potential hydrogen concentra- tion variations on the ^{36}Cl production in the studied samples is assumed to have been negligible during the exposure duration to cosmic ray derived particles of the sampled surfaces. Nonetheless, we here tenta- tively estimate the effect of snow cover on the ^{36}Cl CRE ages of our samples, based on the quantification of the influence of a hydrogen-rich cover on cosmogenic nuclide production rates as a function of the thermal-neutron-related contribution to total nuclide production pro- posed in Fig. 7 of Dunai et al. (2014): conservatively assuming an an- nual snow cover of two months with a thickness of 2.5 cm water equivalent (i.e. a snow thickness of ~10–20 cm) and a 50% thermal- neutron-related ^{36}Cl contribution (i.e. the potential effect from the 20% epithermal-neutron-related ^{36}Cl contribution is ignored for a sample with a 70% ^{36}Cl contribution from low-energy neutrons) would result in ^{36}Cl CRE ages younger by ~12%, which is within the global un- certainties assigned to our ages. As for the rock surface geometry, Zreda et al. (1993) and references herein suggest that the low-energy neutron flux below an

irregularly shaped rock surface might be reduced by up to 30%, due to neutron diffusion out of the rock into air. Thus, the pro- truding and irregular forms of the sampled boulders and tumuli features (section 3.1.1; Fig. 3) might in fact have had an effect on the Cl-related ^{36}Cl production and could therefore explain the differences between the nominal values of samples Pico 4 (3.40 ka), Pico 5 (2.62 ka) and Pico 6 (3.07 ka). The biggest thalli of *Rhizocarpon geographicum* found in the study area, characterized by well-defined and homogeneous size, do not confirm the assumption of Innes (1985) and Matthews and Trenbirth (2011), that they can reach a maximum age of only 500 years. The hypothesis of Miller (1973), Calkin and Ellis (1984) and Benedict (2009) that the thalli of this species can exceed as much as 3000 years, cannot directly be supported, either, with the here presented data. However, assuming that *Rhizocarpon geographicum* can become as old as 3000 years and that the lichen growth was not disturbed by fire or volcanic activity since the emplacement of lava flow B, a possible time lapse between the lava flow emplacement and the beginning of lichen growth, or ecesis interval, of a few hundred years at 4600 m a.s.l. (lava flow "B") might be suggested by the difference between the ^{36}Cl CRE and lichenometric ages. This value is significantly higher than the ecesis interval of 0–3 years proposed by Larocque and Smith (2004) in British Columbia and García Sancho et al. (2011) in Tierra de Fuego. The ecesis time in the study area could be overestimated due to the natural mor- tality of the first colonizers (Loso and Doak, 2006) and also affected by lithology (volcanic rocks retain few water due to their permeability), climate (long dry season, November–April) and repeated volcanic ac- tivity. Thus, due to these biological and local environmental con- straints, the ecesis time of *Rhizocarpon geographicum* of a few hundred years seems too long at Pico de Orizaba. By contrast, the ecesis time of the alpine shrub *Juniperus monticola* is not known and cannot be in- ferred from this work.

6. Conclusions

Three surface dating methods indicate that lava flows previously considered as related to historic (mid 16th to early 17th century) eruptions of Pico de Orizaba are substantially older. Regarding lava flow "A", *in situ*-produced ^{36}Cl CRE dating lead to a ^{36}Cl CRE mean age of 3.03 ± 0.70 ka, dendrochronology based on the alpine shrub *Juniperus monticola* leads to a minimum age of 834 years, while liche- nometry of *Rhizocarpon geographicum* indicates a minimum age of 1130 years. Regarding lava flow "B", *in situ*-produced cosmogenic ^{36}Cl CRE dating lead to a ^{36}Cl CRE mean age of 1.45 ± 0.35 ka and lichenometry leads to an age of ~1000 years. Although dendrochronology and li- chenometry only provide minimum ages compared to ^{36}Cl CRE dating, these two methods bear the potential to directly date lava flows of up to ~800 years using the tree species *Juniperus monticola* and up to ~1000 years using the lichen species *Rhizocarpon geographicum,* respectively. Overall, the combination of *in situ*-produced ^{36}Cl CRE dating, licheno- metry and dendrochronology constitutes a pertinent approach to date young lava flows at high elevation sites where other methods are un- suitable and, thus, to refine the eruptive history of other volcanoes on Earth.

Table 6
Field data and ages of thalli of *Rhizocarpon geographicum* growing on lava flows A and B. The lines high- lighted in green correspond to thalli older than 900 years. Measurements took place in March 2015 and May–June 2016.

Sample	Lava flow	Latitude	Longitude	Altitude (m.a.s.l.)	Diameter (mm)	Age (years)
Site 1.1	Lava A	18.99	-97.30	4144	46	200
Site 1.2	Lava A	18.99	-97.30	4144	42	185
Site 1.3	Lava A	18.99	-97.30	4144	43	190
Site 1.4	Lava A	18.99	-97.30	4144	52	225
Site 1.5	Lava A	18.99	-97.30	4144	67	290
Site 1.6	Lava A	18.99	-97.30	4144	56	245
Site 1.7	Lava A	18.99	-97.30	4144	87	380
Site 2.1 (a)	Lava A	18.99	-97.30	4143	65	285
Site 2.1 (b)	Lava A	18.99	-97.30	4143	58	250
Site 2.2	Lava A	18.99	-97.30	4143	56	245
Site 2.3	Lava A	18.99	-97.30	4143	92	400
Site 2.4	Lava A	18.99	-97.30	4143	51	220
Site 3.1	Lava A	19.00	-97.30	4158	152	660
Site 3.2	Lava A	19.00	-97.30	4158	154	670
Site 3.3	Lava A	19.00	-97.30	4158	127	550
Site 3.4	Lava A	19.00	-97.30	4158	83	360
Site 3.5	Lava A	19.00	-97.30	4158	164	715
Site 4.1	Lava A	19.00	-97.30	4165	143	620
Site 4.2	Lava A	19.00	-97.30	4165	124	540
Site 4.3	Lava A	19.00	-97.30	4165	165	720
Site 4.4	Lava A	19.00	-97.30	4165	75	325
Site 4.5	Lava A	19.00	-97.30	4165	125	545
Site 5.1	Lava B	19.02	-97.27	4935	23	100
Site 5.2	Lava B	19.02	-97.27	4935	26	115
Site 5.3	Lava B	19.02	-97.27	4935	90	390
Site 5.4	Lava B	19.02	-97.27	4935	37	160
Site 6.1	Lava B	19.01	-97.27	4831	37	160
Site 6.2	Lava B	19.01	-97.27	4831	35	150
Site 6.3	Lava B	19.01	-97.27	4831	74	320
Site 6.4	Lava B	19.01	-97.27	4831	83	360
Site 7.1	Lava B	19.01	-97.27	4589	143	620
Site 7.2	Lava B	19.01	-97.27	4589	130	565
Site 7.3	Lava B	19.01	-97.27	4589	98	425
Site 7.4	Lava B	19.01	-97.27	4589	109	475
Site 7.5	Lava B	19.01	-97.27	4589	102	445
Site 8.1	Lava B	19.01	-97.27	4573	215	935
Site 8.2	Lava B	19.01	-97.27	4573	139	605
Site 8.3	Lava B	19.01	-97.27	4573	230	1000
Site 8.4	Lava B	19.01	-97.27	4573	193	840
Site 9.1	Lava B	19.01	-97.28	4577	235	1020
Site 9.2	Lava B	19.01	-97.28	4577	155	675
Site 10.1	Lava B	19.01	-97.28	4576	250	1090
Site 10.2	Lava B	19.01	-97.28	4576	237	1030
Site 11.1	Lava A	19.01	-97.28	4418	155	675
Site 11.2	Lava A	19.01	-97.28	4418	93	405
Site 11.3	Lava A	19.01	-97.28	4418	220	960
Site 11.4	Lava A	19.01	-97.28	4418	100	435
Site 11.5	Lava A	19.01	-97.28	4418	155	675
Site 12.1	Lava A	19.01	-97.28	4448	195	850
Site 13.1	Lava A	19.01	-97.28	4496	120	520
Site 13.2	Lava A	19.01	-97.28	4496	155	675
Site 13.3	Lava A	19.01	-97.28	4496	155	675
Site 13.4	Lava A	19.01	-97.28	4496	120	520
Site 13.5	Lava A	19.01	-97.28	4496	210	915
Site 13.6	Lava A	19.01	-97.28	4496	130	565
Site 13.7	Lava A	19.01	-97.28	4496	150	650
Site 13.8	Lava A	19.01	-97.28	4496	150	650
Site 14.1	Lava A	19.01	-97.29	4400	115	500

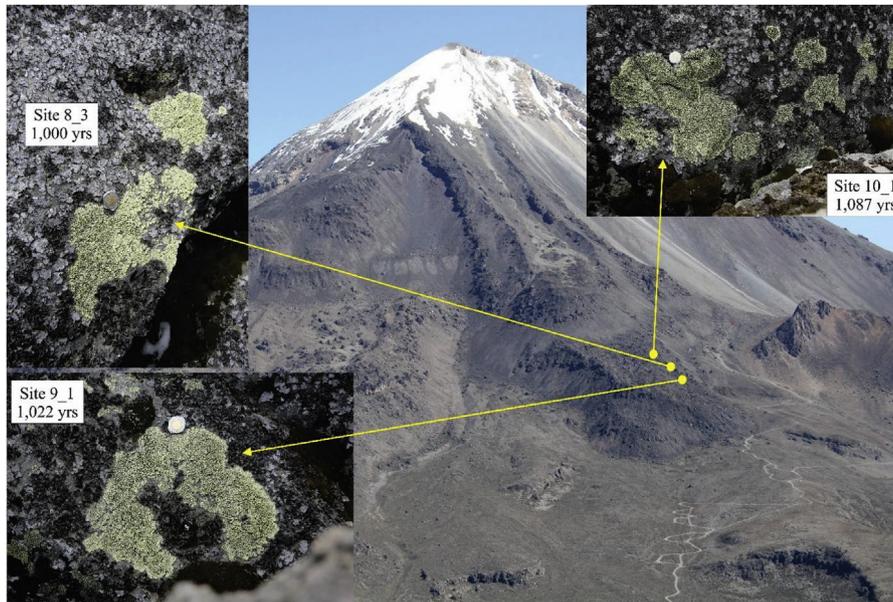| Site 14.2	Lava A	19.01	-97.29	4400	260	1130
Site 14.3	Lava A	19.01	-97.29	4400	140	610
Site 14.4	Lava A	19.01	-97.29	4400	90	390
Site 14.5	Lava A	19.01	-97.29	4400	130	565
Site 14.6	Lava A	19.01	-97.29	4400	155	675

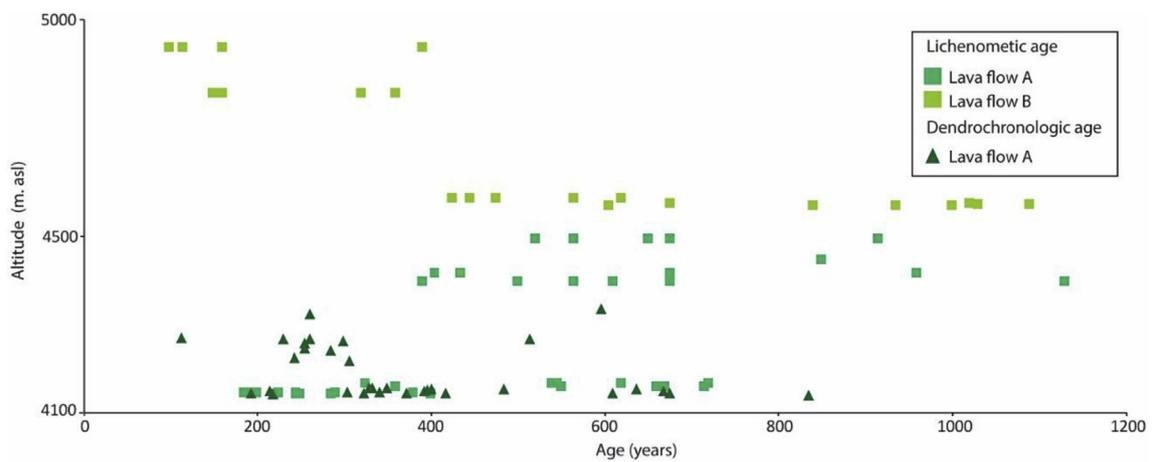Fig. 7. Locations, characteristics and ages of the biggest lichens found on lava flow "B". Three of them lead to an age older than 1000 years.

Fig. 8. Distribution of the ages of *Rhizocarpon geographicum* and *Juniperus monticola* depending on the altitude on lava flows "A" and "B".

Table 7

Ages of the lava flows A and B according to *in situ*-produced ^{36}Cl (arithmetic mean), lichenometry (oldest *Rhizocarpon geographicum*) and dendrochronology (oldest *Juniperus monticola*).

Lava flow	^{36}Cl CRE age (ka)	Lichenometry (ka)	Dendrochronology (ka)
A	3.03 ± 0.70	1.13	0.834
B	1.45 ± 0.35	1.08	–

References

Aciego, M.S., DePaolo, D.J., Kennedy, B.M., Lamb, M.P., Sims, K.W., Dietrich, E., 2007. Combining (^{3}He) cosmogenic dating with U-Th/He eruption ages using olivine in basalt. Earth Planet Sci. Lett. 254, 288–302.

Angiel, P.J., Dąbski, M., 2012. Lichenometric ages of the Little ice age moraines on king George island and of the last volcanic activity on Penguin island (west Antarctica). Geogr. Ann. Phys. Geogr. 94 (3), 395–412.

Armstrong, R.A., 2016. Lichenometric dating (lichenometry) and the biology of the lichen genus Rhizocarpon: challenges and future directions. Geogr. Ann. Phys. Geogr. 98, 183–206.

Arnold, M., Aumaître, G., Bourlès, D.L., Keddadouche, K., Braucher, R., Finkel, R.C., Nottoli, E., Benedetti, L., Merchel, S., 2013. The French accelerator mass spectro- metry facility ASTER after 4 years: status and recent developments on 36Cl and 129I. Nucl. Instrum. Meth. Phys. Res. 294, 24–28.

Balco, G., Stone, J.O., Lifton, N.A., Dunai, T.J., 2008. A complete and easily accessible means of calculating surface exposure ages or erosion rates from ^{10}Be and ^{26}Al measurements. Quat. Geochronol. 3, 174–195.

Bashenina, B., 1977. Geomorphological Mapping. High Level Education. URSS, Moscow (In Russian).

Beget, J.E., 1984. Tephrochronology of late Wisconsin deglaciation and Holocene glacier fluctuations near Glacier Peak, North Cascade range, Washington. Quat. Res. 21 (3), 304–316.

Benedict, J.B., 2009. A review of lichenometric dating and its applications to archaeology. Am. Antiq. 143–172.

Bradwell, T., Armstrong, R.A., 2007. Growth rates of Rhizocarpon geographicum lichens: a review with new data from Iceland. J. Quat. Sci. 2, 311–320.

Briner, J.P., 2011. Dating glacial landforms. In: Encyclopedia of Snow, Ice and Glaciers. Springer, Netherlands, pp. 175–176.

Bull, W.B., 2015. Lichenometry. In: Encyclopedia of Scientific Dating Methods, pp. 372–378 Shington, USA.

Burbank, D.W., 1981. A chronology of late Holocene glacier fluctuations on Mount Rainier, Washington. Arct. Alp. Res. 13 (4), 369–386.

Calkin, P.E., Ellis, J.M., 1984. Development and application of a lichenometric dating curve, Brooks Range, Alaska. Dev. Palaeontol. Stratigr. 7, 227–246.

Calvert, A.T., Moore, R.B., McGeehin, J.P., Rodrigues da Silva, A.M., 2006. Volcanic history and ^{40}Ar/^{39}Ar geochronology of Terceira island, azores, Portugal. J. Volcanol. Geoth. Res. 156, 103–115.

Carrasco-Núñez, G., Rose, W.I., 1995. Eruption of a major Holocene pyroclastic flow at Citlaltépetl volcano (Pico de Orizaba), México, 8.5-9.0 ka. J. Volcanol. Geoth. Res. 69, 197–215.

Carrasco-Núñez, G., 1997. Lava flow growth inferred from morphometric parameters: a case study of Citlaltépetl volcano, Mexico. Geol. Mag. 134, 151–162.

Carrasco-Núñez, G., 2000. Structure and proximal stratigraphy of Citlaltépetl volcano (Pico de Orizaba), Mexico. Geol. Soc. Am. 334, 247–262.

Cerling, T.E., 1990. Dating geomorphologic surfaces using cosmogenic ^{3}He. Quat. Res. 33, 148–156.

Clarkson, B.R., Clarkson, B.D., 1983. Mt. Tarawera: 2. Rates of change in the vegetation and flora of the high domes. New Zealand J. Ecol. 6, 107–119.

Conway, C.E., Townsend, D.B., Leonard, G.S., Wilson, C.J.N., Calvert, A.T., Gamble, J.A., 2015. Lava-ice interaction on a large composite volcano: a case study from Ruapehu, New Zealand. Bull. Volcanol. 77, 21.

Crandell, D.R., Mullineaux, D.R., Sigafoos, R.S., Rubin, M., 1974. Chaos crags eruptions and rockfall-avalanches, Lassen volcanic national park, California. US Geol. Surv. J. Res. 2, 49–59.

Delunel, R., Bourlès, D.L., Van der Beek, P.A., Schlunegger, F., Leya, I., Masarik, J., Paquet, E., 2014. Snow shielding factors for cosmogenic nuclide dating inferred from long-term neutron detector monitoring. Quat. Geochronol. 24, 16–26.

Dunai, T.J., 2010. Cosmogenic nuclides. Principles, Concepts and Applications in the Earth Surface Sciences. Cambridge University Press, pp. 198.

Dunai, T.J., Binnie, S.A., Hein, A.S., Paling, S.M., 2014. The effects of a hydrogen-rich ground cover on cosmogenic termal neutrons: implications for exposure dating. Quat. Geochronol. 22, 183–191.

Dunbar, N.W., 1999. Cosmogenic ^{36}Cl-determined age of the Carrizozo lava flows, south-central New Mexico. N. M. Geol. 21 (2), 25–29.

Espanon, V.R., Honda, M., Chivas, A.R., 2014. Cosmogenic ^{3}He and ^{21}Ne surface exposure dating of young basalts from Southern Mendoza, Argentina. Quat. Geochronol. 19, 76–86.

Fenton, C.R., Niedermann, S., 2014. Surface exposure dating of young basalts (1-200 ka) in the San Francisco volcanic field (Arizona, USA) using cosmogenic ^{3}He and ^{21}Ne. Quat. Geochronol. 19, 87–105.

Fink, D., Vogt, S., Hotchkis, M., 2000. Cross-sections for 36Cl from Ti at Ep =35–150 MeV: applications to in-situ exposure dating. Nucl. Instrum. Methods Phys. Res. Sect. B Beam Interact. Mater. Atoms 172, 861–866.

Foeken, J., Stuart, F.M., Francalanci, L., 2009. Dating Holocene lavas on Stromboli, Italy using cosmogenic He. Quat. Geochronol. 4, 517–524.

Foeken, J., Stuart, F.M., Mark, D.F., 2012. Long-term low latitude cosmogenic ^{3}He pro- duction rate determined from a 126 ka basalt from Fogo, Cape Verdes. Earth Planet Sci. Lett. 359–360, 14–25.

Franco-Ramos, O., Vázquez-Selem, L., Zamorano-Orozco, J.J., Villanueva-Díaz, J., 2017. Edad, dinámica geomorfológica y tipología de barrancas en el sector norte del volcán Popocatépetl, México. Bol. Soc. Geol. Mex. 69, 1–19.

García-Sancho, L., Palacios, D., Green, T.G.A., Vivas, M., Pintado, A., 2011. Extreme high lichen growth rates detected in recently deglaciated areas in Tierra del Fuego. Polar Biol. 34, 813–822.

Germa, A., Quidelleur, X., Gillot, P.Y., Tchilinguirian, P., 2010. Volcanic evolution of the black-arc Pleistocene Payun Matru volcanic field (Argentina). J. S. Am. Earth Sci. 29, 717–730.

Grissino-Mayer, H.D., 2001. Evaluating crossdating accuracy: a manual and tutorial for the computer program COFECHA. Tree-Ring Res. 57 (2), 205–221.

Heineke, C., Niedermann, S., Hetzel, R., Akal, C., 2016. Surface exposure dating of Holocene basalt flows and cinder cones in the Kula volcanic field (Western Turkey) using cosmogenic ^{3}He and ^{10}Be. Quat. Geochronol. 34, 81–91.

Höskuldsson, A., Robin, C., 1993. Late Pleistocene to Holocene eruptive activity of Pico de Orizaba, Eastern Mexico. Bull. Volcanol. 55, 571–587.

Innes, J.L., 1985. An examination of some factors affecting the largest lichens on a sub- strate. Arct. Alp. Res. 17, 99–106.

Ivy-Ochs, S., Synal, H.A., Roth, C., Schaller, M., 2004. Initial results from isotope dilution for Cl and ^{36}Cl measurements at the PSI/ETH Zurich AMS facility. Nucl. Instrum. Methods Phys. Res. Sect. B Beam Interact. Mater. Atoms 223–224, 623–627.

Jomelli, V., Lane, T., Favier, V., Masson-Delmotte, V., Swingedouw, D., Rinterknecht, V., Schimmelpfennig, I., Brunstein, D., Verfaillie, D., Adamson, K., Leanni, L., Mokadem, F., Aumaitre, G., Bourles, D.L., Keddadouche, K., 2016. Paradoxical cold conditions during the medieval climate anomaly in the Western Arctic. Sci. Rep. 6, 32984. http://dx.doi.org/10.1038/srep32984.

Kirkbride, M.P., Dugmore, A.J., 2008. Two millennia of glacier advances from southern Iceland dated by tephrochronology. Quat. Res. 70 (3), 398–411.

Koch, J., Clague, J.J., Osborn, G.D., 2007. Glacier fluctuations during the past millennium in Garibaldi provincial park, southern coast mountains, British Columbia. Can. J. Earth Sci. 44, 1215–1233.

Kurina, L.M., Vitousek, P.M., 1999. Controls over the accumulation and decline of a ni- trogen-fixing lichen, Stereocaulon vulcani, on young Hawaiian lava flows. J. Ecol. 87 (5), 784–799.

Kurz, M.D., Rowland, S.K., Curtice, J., Saal, A.E., Naumann, T., 2014. Eruption rates for Fernandina volcano: a new chronology at the Galápagos hotspot center. In: The Galapagos: a Natural Laboratory for the Earth Sciences, Geophysical Monograph 204, first ed. American Geophysical Union.

Larocque, S.J., Smith, D.J., 2004. Calibrated Rhizocarpon spp. Growth curve for the mount Waddington area, British Columbia coast mountains, Canada. Arctic Antarct. Alpine Res. 36, 407–418.

Lauer, W., 1978. Timberline studies in Central Mexico. Arct. Alp. Res. 10, 383–396.

Le Bas, M.J., Le Maitre, R.W., Streckeisen, A., Zanettin, B., 1986. A chemical classification of volcanic rocks based on the total alkali-silica diagram. J. Petrol. 27, 745–750.

Lescinsky, D.T., Fink, J.H., 2000. Lava and ice interaction at stratovolcanoes: use of

characteristic features to determine past glacial extents and future volcanic hazards. J. Geophys. Res. 105, 23,711–23,726.

Loso, M.G., Doak, D.F., 2006. The biology behind lichenometric dating curves. Oecologia 147, 223–229.

Mancebo, J.M.G., Pinto, L.S., Tejera, E.B., Lima, A.L., 1989. Contribución al estudio florístico de las coladas históricas de las Islas Canarias. I: chinyero (Tenerife). An. del Jardín Botánico Madr. 46 (2), 437–444.

Marrero, S.M., Phillips, F.M., Caffee, M.W., Gosse, J.C., 2016. CRONUS-Earth cosmogenic ^{36}Cl calibration. Quat. Geochronol. 31, 199–219.

Masarik, J., Kim, K.J., Reedy, R.C., 2007. Numerical simulations of in situ production of terrestrial cosmogenic nuclides. Nucl. Instrum. Methods Phys. Res. Sect. B Beam Interact. Mater. Atoms 259, 642–645.

Matthews, J.A., Trenbirth, H.E., 2011. Growth rate of a very large crustose lichen (Rhizocarpon subgenus) and its implications for lichenometry. Geogr. Ann. Phys. Geogr. 93 (1), 27–39.

Medynski, S., Pik, R., Burnard, P., Vye-Brown, C., France, L., Schimmelpfennig, I., Whaler, K., Johnson, N., Benedetti, L., Ayelew, D., Yirgu, G., 2015. Stability of rift axis magma reservoirs: spatial and temporal evolution of magma supply in the Dabbahu rift segment (Afar, Ethiopia) over the past 30 kyr. Earth Planet Sci. Lett. 409, 278–289.

Miller, G.H., 1973. Late quaternary glacial and climatic history of northern cumberland peninsula, Baffin island, NWT, Canada. Quat. Res. 3 (4), 561–583.

N.O.A.A, 1976. U.S. Standard Atmosphere. US Gov. Print. Off.

O'Neal, M.A., Schoenenberger, K.R., 2003. A Rhizocarpon geographicum growth curve for the Cascade Range of Washington and northern Oregon, USA. Quat. Res. 60, 233–241.

O'Neal, M.A., Legg, N.T., Hanson, B., Morgan, D.J., Rothgeb, A., 2013. Lichenometric dating of rock surfaces in the northern Cascade Range, USA. Geogr. Ann. Phys. Geogr. 95, 241–248.

Palacios, L., García-Sancho, Zamorano, J.J., Andrés, N., Pintado, A., 2012. The degla- ciation of Iztaccíhuatl volcano (Mexico) from the Little Ice Age maximum to the present, determined by photogrametry and lichenometry. Geophys. Res. Abstr. 14, EGU2012–3755 2012.

Phillips, F.M., Stone, W.D., Fabryka-Martin, J.T., 2001. An improved approach to cal- culating low-energy cosmic-ray neutron fluxes near the land/atmosphere interface. Chem. Geol. 175, 689–701.

Pierson, T.C., 2007. Dating young geomorphic surfaces using age of colonizing Douglas fir in southwestern Washington and northwestern Oregon, USA. Earth Surf. Process. Landforms 32, 811–831.

Porter, S.C., 1981. Lichenometric studies in the cascade range of Washington: establish- ment of Rhizocarpon geographicum growth curves at mount Rainier. Arct. Alp. Res. 13 (1), 11–23.

Renne, P.R., 2000. K-ar and ^{40}Ar/^{39}Ar Dating. Quaternary Geochronology: Methods and Applications. American Geophysical Union.

Robinson, W.J., Evans, R., 1980. A microcomputer-based tree ring measuring system. Tree-Ring Bull. 40, 59–64.

Rodriguez-Ramírez, A., Caballero, M., Roy, P., Ortega, B., Vázquez-Castro, G., Lozano-García, S., 2015. Climatic variability and human impact during the last 2000 years in western Mesoamerica: evidence of late Classic (AD 600-900) and Little Ice Age drought events. Clim. Past 11, 1239–1248.

Rossotti, A., Carrasco-Núñez, G., 2004. Stratigraphy of the 8.5-9.0 ka B.P. Citlaltépetl pumice fallout sequence. Rev. Mex. Ciencias Geol. 21, 353–370.

Schimmelpfennig, I., 2009. Cosmogenic ^{36}Cl in Ca and K Rich Minerals: Analytical Developments, Production Rate Calibrations and Cross Calibration with ^{3}He and ^{21}Ne.

Ph.D. Thesis. Paul Cezanne Aix-Marseille III University, Aix en Provence, France.

Schimmelpfennig, I., Benedetti, L., Finkel, R., Pik, R., Blard, P.H., Bourle, D., Burnard, P., Williams, A., 2009. Sources of in-situ 36Cl in basaltic rocks. Implications for cali- bration of production rates. Quat. Geochronol. 4, 441–461.

Schimmelpfennig, I., Benedetti, L., Garreta, V., Pik, R., Blard, P.H., Burnard, P., Bourlès, D., Finkel, R., Ammon, K., Dunai, T., 2011. Calibration of cosmogenic ^{36}Cl production rates from Ca and K spallation in lava flows from Mt. Etna (38ºN, Italy) and Payun Matru (36ºS, Argentina). Geochem. Cosmochim. Acta 75, 2611–2632.

Schimmelpfennig, I., Schaefer, J.M., Akcar, N., Koffman, T., Ivy-Ochs, S., Schwartz, R., Finkel, R.C., Zimmerman, S., Schlüchter, C., 2014. A chronology of Holocene and Little Ice Age glacier culminations of the Steingletscher, Central Alps, Switzerland, based on high-sensitivity beryllium-10 moraine dating. Earth Planet Sci. Lett. 393, 220–230.

Schneider, B., Kuiper, K.F., Mai, K., Foeken, J.P.T., Stuart, F.M., Wijbrans, 2014. Fuerteventura - assessment of a calibration site for cosmogenic ^{3}He exposure dating with the ^{40}Ar/^{39}Ar incremental heating method. Quat. Geochronol. 21, 58–69.

Sharma, P., Kubik, P.W., Fehn, U., Gove, H.E., Nishiizumi, K., Elmore, D., 1990. Development of ^{36}Cl standards for AMS. Nucl. Instrum. Meth. Phys. Res. 52, 410–415.

Shimizu, A., 2004. Community structure of lichens in the volcanic highlands of Mt. Tokachi, Hokkaido, Japan. Bryol. 107 (2), 141–151.

Shroder Jr., J.F., Butler, D.R., 1987. Tree ring analysis in the earth sciences. In: Jacoby Jr.G.C., Hornbeck, J.W. (Eds.), Proceedings of the International Symposium on Ecological Aspects of Tree-ring Analysis, Publication CONF-8608144. U.S. Department of Energy, Tarrytown, New York, pp. 186–212.

Siebe, C., Abrams, M., Sheridan, M.F., 1993. Major Holocene block-and-ash fan at the western slope of ice-capped Pico de Orizaba volcano, México: implications for future hazards. J. Volcanol. Geoth. Res. 59, 1–33.

Simonov, Yu G., 1972. Regional Geomorphological Analysis. Gos. Uni, Moscow: Mosk (In Russian).

Stokes, M.A., Smiley, T.L., 1968. An Introduction to Tree-ring Dating. The University of Arizona Press, Tucson, Arizona 73 pp.

Stone, J., 2000. Air pressure and cosmogenic isotope production. J. Geophys. Res. 105, 23,753–23,759.

Stone, J.O., Fifield, K., Vasconcelos, P., 2005. Terrestrial chlorine-36 production from spallation of iron. In: 10th International Conference on Accelerator Mass Spectrometry, Berkeley, USA.

Stoffel, M., Bollschweiler, M., Butler, D.R., Luckman, B.H., 2010. Tree rings and natural hazards-an introduction. In: Stoffel, M., Bollschweiler, M., Butler, D.R., Luckman, B.H. (Eds.), Tree Rings and Natural Hazards: a State-of-the-art. Springer, Heidelberg, New York, pp. 495–502.

Talbot, S.S., Talbot, S.L., Walker, L.R., 2010. Post-eruption legacy effects and their im- plications for long-term recovery of the vegetation on Kasatochi Island, Alaska. Arctic Antarct. Alpine Res. 42 (3), 285–296.

Trumbore, S.E., 2000. Radiocarbon Geochronology. Quaternary Geochronology: Methods and Applications. American Geophysical Union.

Uppala, S.M., KÅllberg, P.W., Simmons, A.J., Andrae, U., Bechtold, V.D.C., Fiorino, M., Gibson, J.K., Haseler, J., Hernandez, A., Kelly, G.A., Li, X., Onogi, K., Saarinen, S.,

Sokka, N., Allan, R.P., Andersson, E., Arpe, K., Balmaseda, M.A., Beljaars, A.C.M., Van De Berg, L., Bidlot, J., Bormann, N., Caires, S., Chevallier, F., Dethof, A., Dragosavac, M., Fisher, M., Fuentes, M., Hagemann, S., Ho_lm, E., Hoskins, B.J., Isaksen, L., Janssen, P.A.E.M., Jenne, R., Mcnally, A.P., Mahfouf, J.-F., Morcrette, J.-J., Rayner, N.A., Saunders, R.W., Simon, P., Sterl, A., Trenberth, K.E., Untch, A., Vasiljevic, D., Viterbo, P., Woollen, J., 2005. The ERA-40 Re-analysis. vol. 131. Quartely Journal of the Royal Meteorological Society, pp. 2961–3012. https://doi. org/10.1256/qj.04.176.

Vázquez-Selem, L., Heine, K., 2011. Late quaternary glaciation in Mexico. In: Ehlers, J., Gibbard, P.L., Hughes, P.D. (Eds.), Quaternary Glaciations - Extent and Chronology. A Closer Look. Elsevier, Amsterdam, pp. 849–861. http://doi.org/10.1016/B978-0- 444-53447-7.00061-1.

Vermeesch, P., 2007. CosmoCalc: an excel add-in for cosmogenic nuclide calculations. G-cubed 8, 1525–2027.

Villanueva-Díaz, J., Cerano, J., Vázquez Selem, L., Stahle, D.W., Fulé, P.Z., Yocom, L.L., Franco-Ramos, O., Ruiz Corral, J.A., 2015. Red dendrocronológica del pino de altura (Pinus hartwegii Lindl.) para estudios dendroclimáticos en el noreste y centro de México, vol. 86. Investigaciones Geográficas. Boletín del Instituto de Geografía, UNAM, pp. 5–14.

Villanueva-Díaz, J., Vázquez-Selem, L., Gómez-Guerrero, A., Cerano-Paredes, J., Aguirre-González, N.A., Franco-Ramos, O., 2016. Dendrochronologic potential of *Juniperus monticola* Martínez in mount Tláloc, México. Rev. Fitotec. Mex. 39 (2), 175–185 ISSN 0187-7380.

Ward, G.K., Wilson, S.R., 1978. Procedure for comparing and combining radiocarbon age determinations: a critique. Archaeometry 20, 19–31.

Wijbrans, J., Schneider, B., Kuiper, K., Calvari, S., Branca, S., De Beni, E., Norini, G., Corsaro, R.A., Miraglia, L., 2011. ^{40}Ar/^{39}Ar geochronology of Holocene basalts; ex- amples from Stromboli, Italy. Quat. Geochronol. 6, 223–232.

Zotz, G., 2017. Growth of Rhizocarpon geographicum in the summit region of volcán Barú, Panamá. Lichenol. 49, 535–538.

Zreda, M.G., Phillips, F.M., Kubik, P.W., Sharma, P., Elmore, D., 1993. Cosmogenic ^{36}Cl dating of a young basaltic eruption complex, Lathrop Wells, Nevada. Geology 21, 57–60.

Zweck, C., Zreda, M., Desilets, D., 2013. Snow shielding factors for cosmogenic nuclide dating inferred from Monte Carlo neutron transport simulations. Earth Planet Sci. Lett. 379, 64–71.